Substrate grain size and orientation of Cu and Cu–Ni foils used for the growth of graphene films

Zachary R. Robinson, Parul Tyagi, Thomas M. Murray, and Carl A. Ventrice Jr.[a)]
College of Nanoscale Science and Engineering, University at Albany–SUNY, 257 Fuller Road, Albany, New York 12203

Shanshan Chen, Andrew Munson, Carl W. Magnuson, and Rodney S. Ruoff[b)]
Department of Mechanical Engineering and Materials Science and Engineering Program, The University of Texas at Austin, 1 University Station C2200, Austin, Texas 78712

(Received 8 August 2011; accepted 27 October 2011; published 2 December 2011)

Graphene growth on Cu foils by catalytic decomposition of methane forms predominantly single-layer graphene films due to the low solubility of carbon in Cu. On the other hand, graphene growth on Cu–Ni foils can result in the controlled growth of few-layer graphene films because of the higher solubility of carbon in Ni. One of the key issues for the use of graphene grown by chemical vapor deposition for device applications is the influence of defects on the transport properties of the graphene. For instance, growth on metal foil substrates is expected to result in multidomain graphene growth because of the presence of grains within the foil that exhibit a variety of surface terminations. Therefore, the size and orientation of the grains within the metal foil should influence the defect density of the graphene. For this reason, we have studied the effect of total anneal time and temperature on the orientation and size of grains within Cu foils and Cu–Ni alloy foils with a nominal concentration of 90/10 by weight. The graphene growth procedure involves preannealing the foil in a H_2 background followed by the graphene growth in a CH_4/H_2 atmosphere. Measurements of the substrate grain size have been performed with optical microscopy and scanning electron microscopy. These results show typical lateral dimensions ranging from a few millimeters up to approximately a centimeter for Cu foils annealed at 1030 °C for 35 min and from tens of microns up to a few hundred microns for the 90/10 Cu–Ni foils annealed at 1050 °C for times ranging from 45 to 90 min. The smaller grains within the Cu–Ni foils are attributed to the higher melting point of the Cu–Ni alloy. The crystallographic orientation within each substrate grain was studied with electron backscatter diffraction, and shows that the preferred orientation for the Cu foil is primarily toward the (100) surface plane. For the 90/10 Cu–Ni foils, the orientation of the surface of the grains is initially toward the (110) plane and shifts into an orientation midway between the (100) and (111) planes as the anneal time is increased. © *2012 American Vacuum Society*. [DOI: 10.1116/1.3663877]

I. INTRODUCTION

Graphene, which is a single atomic layer of sp^2-hybridized carbon, has attracted quite a bit of interest within the scientific community because of its unique mechanical, thermal, optical, and electrical properties.[1–3] For instance, measurements of the fracture strength of exfoliated graphene flakes yield a value of ~125 GPa,[4] which is over 200 times larger than what has been measured for single fibers of Kevlar.[5] One of the main reasons that single atomic layers of graphene with areas that are several square centimeters can be isolated and transferred from one substrate to another is because of the high fracture strength of graphene. The current interest in graphene has primarily been motivated by its unique electrical properties. Carrier mobilities as high as 200 000 cm^2/Vs have been reported for suspended single-layer graphene films isolated by micromechanical exfoliation from graphite.[6] In addition, the electronic structure of graphene depends on the number of graphene layers and the stacking sequence between the layers.[7] Single-layer graphene is a semimetal with a linear energy dispersion near the Dirac point, which results in a very small effective mass for the carriers.[8–10] On the other hand, a small energy gap can be present in bilayer graphene,[11,12] and few-layer graphene films have electrical properties that differ from single- and bi-layer graphene films and bulk graphite.[7,13]

For most device applications it is important to be able to grow wafer-sized areas of graphene with a controlled number of graphene layers. Although the technique of micromechanical exfoliation of graphene from bulk graphite produces very high quality flakes that are often used to measure its basic physical properties, the typical lateral size of these flakes is much less than a millimeter. A common technique used to fabricate large-area graphene samples is by thermal decomposition of SiC in vacuum.[14–16] The vapor pressure of Si is much higher than that of carbon, therefore, an enrichment of the carbon concentration at the surface region will result at elevated temperatures. This process produces an interfacial carbon layer with partial sp^3 character and one or more sp^2 bonded graphene layers that form above the interfacial layer. One of the main advantages of this

[a)]Electronic mail: cventrice@albany.edu
[b)]Electronic mail: r.ruoff@mail.utexas.edu

growth technique is that the graphene is formed directly on an insulating substrate, which is desirable for most device applications. However, device quality SiC wafers are very expensive, and it is currently difficult to control the uniformity and the number of graphene layers.[17,18]

One of the most promising methods of producing large-area graphene for device applications is by the catalytic decomposition of hydrocarbon molecules on metal foil substrates. By using a polymer-assisted transfer process, these films can often be transferred to insulating or semiconducting substrates, simultaneously maintaining the structural integrity of the graphene. The substrate that has received the most attention for large-area single-layer graphene growth is Cu.[19–23] This is because the solubility of carbon in Cu is negligible at the growth temperatures typically used for graphene growth, which can result in the formation of films that self-terminate at a monolayer when methane is used as the precursor. Because of the low solubility, there is very little carbon in the subsurface region and thus no precipitation of carbon to the surface during the cooling phase.[20] After the formation of a complete monolayer, the growth process stops as graphene is not catalytically active toward the decomposition of methane at these temperatures. For the controlled growth of graphene films that are more than one atomic layer thick, alloys of Cu and Ni can be used[24–26] as the solubility of carbon in Ni at the temperatures typically used for graphene growth is much higher than that of Cu.[27]

For most device applications, it is crucial to maintain a low defect density within the graphene, simultaneously keeping the thickness of the graphene film uniform. Therefore, it is important to be able to develop techniques for growing graphene films that are composed of macroscopic-sized grains as it is expected that a graphene film composed of relatively small grains will have a low carrier mobility due to scattering at the grain boundaries.[28] One of the factors that is expected to influence the grain size within the graphene overlayer is the surface termination and orientation of the metal substrate atoms. For growth on a face-centered cubic (fcc) metal substrate, the preferred orientation should be the (111) surface termination as both this surface and the honeycomb structure of graphene have a hexagonal symmetry. However, most of the studies of graphene growth on Cu have been performed on metal foils that were formed by a cold-rolling process. The primary reason for the use of foils instead of single crystals is to maintain a relatively low-cost method of producing large-area graphene as the size of the substrate dictates the size of the graphene film. Because of the polycrystalline nature of cold-rolled foil substrates, it is important to understand the evolution of the substrate grain size and orientation under typical graphene growth conditions if techniques for growing large-area graphene films with low defect density are to be developed.

A. Low-energy surfaces of fcc metal crystals

Both Cu and Ni crystallize in the simple fcc crystal structure. They have similar lattice constants (3.61 and 3.52 Å for Cu and Ni, respectively) and form a continuous range of solid solutions. The three lowest surface energy terminations of fcc crystals are the (100), (110), and (111) surfaces. The relationship between the bulk lattice constant a_0 and the surface lattice constants a_s and b_s for each surface termination are given in Table I. The relative surface energy for each termination can be estimated by comparing the number of missing nearest neighbors per unit area at each surface.[29] Although this is a relatively simple model that neglects kinetic and other material-specific effects, it can serve as a guide for estimating the relative energies of the low-index surface terminations of fcc crystals. For fcc metals, each atom in the bulk has 12 nearest neighbors. By definition, the atoms at the surface of the metal will be missing some of these nearest neighbors, and thus the energy of the surface atoms will be higher than those in the bulk. For a (100) terminated surface, each surface atom will be missing four nearest neighbors. For a (111) terminated surface, only three nearest neighbors will be missing, and for a (110) terminated surface, six will be missing from each surface atom. As the atomic density of each surface orientation is different, this must be considered when determining the relative surface energies. The total surface energy will be proportional to the factor

TABLE I. Surface terminations of fcc metals.

Metal	a_s	b_s	γ (deg)
fcc(100)	$\frac{1}{\sqrt{2}}a_0$	$\frac{1}{\sqrt{2}}a_0$	90
fcc(110)	$\frac{1}{\sqrt{2}}a_0$	a_0	90
fcc(111)	$\frac{1}{\sqrt{2}}a_0$	$\frac{1}{\sqrt{2}}a_0$	120

$$E_{hkl} = \frac{\text{Number of missing bonds}}{\text{Area of unit cell}}. \quad (1)$$

Therefore, the (111) surface energy factor will be $E_{111} = 12/\sqrt{3}a_0^2$, whereas the other surface energy factors will be $E_{100} = 8/a_0^2$ and $E_{110} = 6\sqrt{2}/a_0^2$. Neglecting next-nearest-neighbor interactions means that the (100) and (110) surfaces are expected to have 15% and 22% higher energies than the (111) surface, respectively. For cold-rolled foils of fcc metals, the plastic deformation of the metal during the rolling process typically results in microscopic grains with a combination of a (100) and (111) texture and considerable disorder.[30] The initial orientation of the grains and the internal stress within the foil are expected to influence the evolution of the grain size and orientation during annealing.

B. Graphene growth on Cu and Cu–Ni surfaces

Graphene crystallizes in the honeycomb structure, which is a hexagonal lattice with a two-atom basis. The symmetry of the (111) surface of a fcc crystal is also hexagonal, whereas the symmetries of the (100) and (110) surfaces are square and rectangular, respectively. From symmetry

arguments alone, it is expected that graphene growth on the (111) surface should result in an overlayer with the fewest rotational domains. The lattice mismatch between the overlayer and substrate can also be an important factor for producing films with low defect density. Both the Cu(111) and Ni(111) surfaces are reasonably well lattice-matched to graphene (−3.7% and −1.2%, respectively). The strength of the overlayer/substrate interaction must also be considered. For systems with only a small lattice mismatch, a strong interaction can result in a pseudomorphic growth (i.e., the strain in the overlayer causes the overlayer to adopt the lattice constant of the substrate). On the other hand, a weak interaction will allow the overlayer to slip in and out of phase with the substrate during growth, resulting in a large coincidence lattice and a "Moiré pattern" type of growth.

The process of grain growth in the foil substrates at elevated temperatures is expected to follow a two-step process. As an unannealed metal foil will exhibit quite a bit of disorder following the cold-rolling process, the first step would be for the ordered regions of the foil to incorporate atoms from the disordered regions during the annealing process. This will result in the formation of a network of connected grains. The second step would be the growth of large grains at the expense of the smaller grains, eventually resulting in the formation of a few grains with macroscopic dimensions. This coalescence of grains is expected to proceed at a much slower rate than the initial nucleation process. However, as the temperature is increased to a value close to the melting point of the metal, the diffusion coefficient of the atoms within the foil will become very large, resulting in the growth of grains with macroscopic dimensions over relatively short time scales. The melting point of Cu is 1083 °C and of Ni is 1453 °C. The melting point of Cu–Ni alloys varies approximately linearly from 1083 to 1453 °C as the atomic concentration of Ni increases from 0% to 100%.[27] As graphene growth on Cu using a methane precursor has typically been performed at ~1000 °C, macroscopic Cu grains should be observed for the foil substrates following relatively short anneals. However, grain growth for Cu–Ni alloy substrates should be slower at the same temperature because of their higher melting points.

The temperature dependence of the vapor pressure of the substrate can also have an influence on the growth rate and orientation of the substrate grains. At 1000 °C, the vapor pressure of Cu and Ni are 6×10^{-5} and 1×10^{-7} Torr, respectively.[31] The flux of atoms impinging on a surface within the molecular flow regime ($P < 10^{-3}$ Torr for a cylindrical tube furnace with a diameter of a few centimeters) is given by

$$\Phi = 3.5 \times 10^{22} \frac{P}{\sqrt{MT}} (\text{atoms/cm}^2\text{s}), \tag{2}$$

where P is the pressure (Torr), M is the molecular weight (g/mol), and T is the temperature (degrees Kelvin).[32] As the rate at which atoms impinge and desorb from a surface is the same at equilibrium, the desorption rate can be found by dividing the flux by the atomic density of the surface. Therefore, the rate at which atoms leave a surface when there is no incident flux is given by

$$\dot{\eta} = \frac{\Phi}{\sigma} (\text{monolayers/s}), \tag{3}$$

where σ is the atomic density (atoms/cm^2). For the Cu(111) surface, this results in a loss of 4 monolayers (ML) of Cu per second from the surface at 1000 °C under ultrahigh vacuum conditions, whereas the sublimation rate from a Ni(111) surface will only be 7×10^{-3} ML/s. For graphene growth on Cu substrates by catalytic decomposition of hydrocarbon molecules, the pressure of the source gas is typically in the mTorr or higher pressure range, which should slow the sublimation rate of Cu from the surface. In addition, if the sample is annealed in a hot-wall reactor, there may be an additional flux of metal atoms impinging on the substrate surface that had previously deposited on the reactor walls. Once graphene growth is initiated, it is expected that the graphene covered regions of the surface will suppress sublimation of the metal substrate atoms.

II. EXPERIMENT

A. Growth of graphene films

The graphene films were grown on Cu and Cu–Ni alloy foils. The Cu foils were purchased from Alfa Aesar and had a purity of 99.8%. An assay for these foils was not available from the manufacturer. The thickness of Cu foils was 25 μm. The Cu–Ni foils were supplied by Midwest Metals, Inc. and had a thickness of 0.005 in. (127 μm). The assay provided by the manufacturer reports concentrations of 88.00% Cu, 9.90% Ni, 1.54% Fe, 0.44% Mn, and 0.10% Zn by weight, with trace amounts of other elements.

The graphene was grown by chemical vapor deposition using methane as the precursor. A hot-wall reactor was used for the growth of the graphene films. It consists of a quartz tube with the reaction zone being heated using radiant heat. The base pressure of the hot-wall reactor was 20 mTorr. The cooling of the sample to room temperature after growth took several hours because of the large thermal mass of the reactor.

The general procedure for growing the graphene films involves annealing the foils in a H_2 atmosphere to reduce the surface oxide and to enlarge the substrate grain size, followed by the introduction of CH_4. As trace amounts of residual oxygen may be present in the reactor, the growth of the graphene was done in a H_2/CH_4 atmosphere to prevent the formation of copper oxide at regions of incomplete graphene growth. The same gas mixture was used during the subsequent cool down to prevent the loss of carbon from the graphene overlayer (e.g., formation of CO and CO_2), which can occur at temperatures higher than ~300 °C. The Cu foils were annealed at 1035 °C in 40 mTorr of H_2 for 30 min, followed by the introduction of CH_4 for a total pressure of 145 mTorr. The graphene growth proceeded for 5 min before initiating the cool down of the sample. The 90/10 Cu–Ni foils were annealed at 1050 °C in 45 mTorr of H_2 for 40 min,

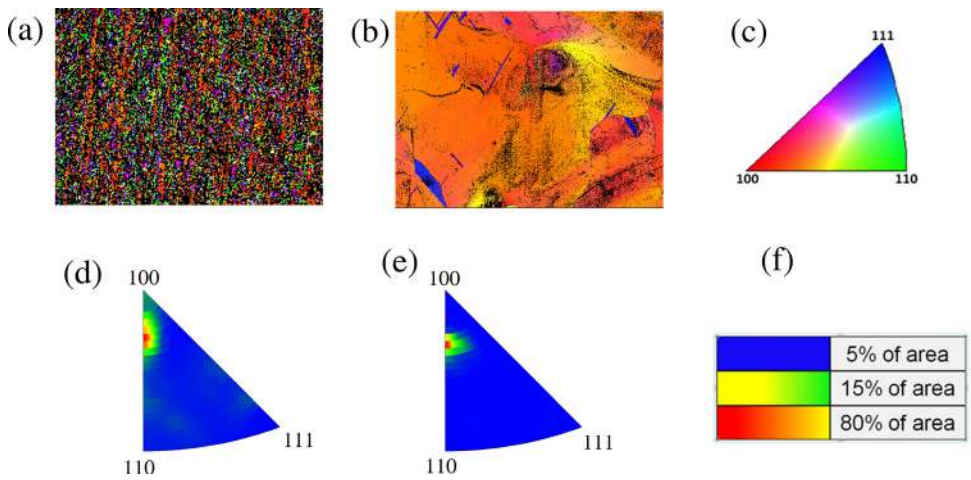

FIG. 1. (Color online) EBSD images of (a) the unannealed Cu foil (1.4 mm × 1.1 mm), (b) the Cu foil after anneal at 1035 °C for 30 min in 40 mTorr H_2 followed by 5 min in 145 mTorr CH_4 (2.5 mm × 1.9 mm), and (c) the EBSD legend. Corresponding inverse pole figures for (d) the unannealed Cu foil, (e) the Cu foil after graphene growth, and (f) the density map of the relative areas. Orientations are with respect to the surface normal, and the color map indicates the percent area that is covered by grains with that particular orientation.

followed by the introduction of CH_4 for a total pressure of 150 mTorr. Growth times for the 90/10 Cu–Ni foils ranging from 5 to 50 min before cool down of the sample.

These methods of growing graphene have been shown previously to result in large-area, continuous, single-layer or few-layer graphene films, depending on the substrate alloy concentration.[19–23,25,26] To monitor the defect density, uniformity, and thickness of the graphene overlayers, X-ray photoelectron spectroscopy (XPS) and Raman spectroscopy were performed on each sample. The results of those measurements will be published elsewhere.[26]

B. SEM and EBSD measurements

The size and shape of the substrate grains were monitored using optical microscopy and high resolution scanning electron microscopy (SEM). Two instruments were used for the SEM measurements: a LEO 1550 SEM and a FEI Nova Nanolab 600 dual beam SEM/focused ion beam (FIB) system. Images were taken with a primary beam ranging from 2 to 5 keV. The crystallographic orientation of the substrate grains was measured with electron backscatter diffraction (EBSD) using an HKL Nordlys detector in the FEI SEM/FIB. For the EBSD measurements, a 30 keV electron beam with ~1 nA of intensity was incident on the sample at an angle of 70°. The electrons penetrate ~5 nm into the surface of the sample, diffract, and form a Kikuchi pattern on a detector positioned a few millimeters from the sample surface.[33] For each pixel, the FLAMENCO® program compares the measured Kikuchi pattern to a library of patterns for crystalline Cu and assigns an orientation. As Cu and Ni are fcc crystals with similar lattice constants and identical core electron structures, it was only necessary to use the pure Cu library for the orientation assignment of the Cu–Ni foils. To perform a complete mapping, the electron beam was rastered over the region of interest in a pixel-by-pixel fashion. The accuracy of the orientation assigned during the EBSD measurements is estimated to be within ±5°. This uncertainty results partially from the difficulty in mounting the foils perfectly flat on the SEM sample stage and also from the spatial resolution of the detector. For instance, an EBSD measurement of a Cu(111) single crystal resulted in an orientation distribution with a half-width of 2°.

III. RESULTS

A. Unannealed Cu and Cu–Ni Foils

For the Cu foil and the 90/10 Cu–Ni foil, EBSD measurements were taken before annealing in H_2. For the Cu–Ni foil, the software could only identify a grain orientation for less than 2% of the surface area within any scan. As our XPS measurements of the as-received Cu–Ni foil provides evidence that the surface region of these samples is heavily oxidized,[26] the lack of crystallographic determination by EBSD for this foil is most likely the result of a disordered native oxide at the surface. However, this could also result from disorder within the alloy below the native oxide or from randomly ordered grains that have a lateral dimension smaller than the probe area of the electron beam (~10 nm).

For the as-received Cu foil, the EBSD software was able to map over 40% of the surface area within a scan onto one of the crystallographic directions of Cu, as shown in Fig. 1(a). The black pixels correspond to areas where the software could not determine a grain orientation within the spot size of the electron beam. Our XPS results show some oxidation at the surface of the pure Cu foils, but to a lesser degree than for the Cu–Ni foils.[26] As with the Cu–Ni foils, the regions with unidentified orientations could result from the disordered native oxide, disorder within the unoxidized Cu, or regions with very small Cu grains with random orientation. The density scale, which identifies the crystallographic orientation relative to the surface normal within each pixel, is shown in Fig. 1(c). There is a large range of crystallographic orientations identified in the EBSD scan [Fig. 1(a)], and the lateral dimensions of the grains are mostly less than 50 μm in size. The grains are also somewhat

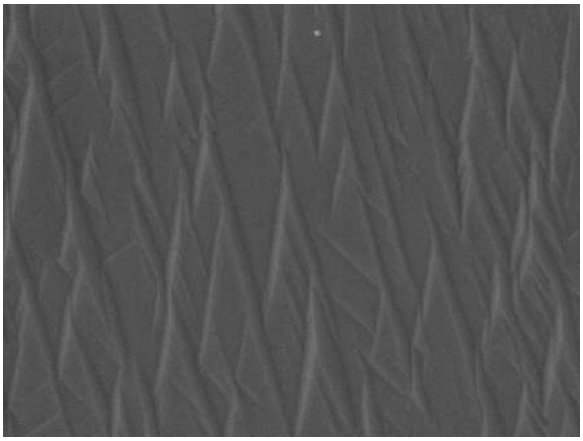

FIG. 2. SEM image of the Cu foil after graphene growth at 1035 °C. Image taken at 5 kV with a 3 mm working distance (3.3 μm × 2.5 μm).

elongated, which is expected for a foil formed by cold-rolling. Statistical analysis of the EBSD map for the pure Cu foil indicates a preference for the surface normal of the grains within the as-received foil to be oriented toward the [100] direction. This can be seen in Fig. 1(d), which is an inverse pole figure (IPF) of the as-received Cu foil.

B. Cu foil after graphene growth

After growth of the graphene overlayer, the typical lateral dimension of the grains within the Cu foil ranged from a few millimeters to as large as a centimeter, as observed with optical microscopy and SEM. This result is reasonable considering the fact that the foil was annealed very close to the melting temperature of Cu during the growth process. An EBSD map of the Cu foil after graphene growth is shown in Fig. 1(b) and reveals that the surface is predominantly (100) terminated. After graphene growth, the EBSD software was able to map over 90% of the surface area within a scan onto one of the crystallographic directions of Cu. The grain orientation relative to the surface normal of the foil is ∼15° from the [100] direction, tilted toward the [110] direction, as can be seen from the IPF in Fig. 1(e). There are also some small (111) oriented inclusions in the Cu foil. A SEM image of the surface is shown in Fig. 2 and reveals a faceted surface, which is expected for a crystal whose surface is misaligned by several degrees from one of the low-energy terminations (in this case, the (100) termination).

TABLE II. Grain evolution for 90/10 Cu–Ni foils at 1050 °C. Columns 2 and 3 represent the percent of the foil covered by grains larger than 20000 and 50000 μm^2, respectively.

Anneal time (min)	20000 μm^2	50000 μm^2
45	50%	18%
65	58%	22%
90	64%	31%

C. Cu–Ni foils after graphene growth

The grain size and orientation within the Cu–Ni foils after graphene growth was found to be much different than that of the Cu foils. The melting point of the 90/10 Cu–Ni alloy foil is estimated to be 1140 °C from the Cu–Ni phase diagram,[27] which is almost 90 °C higher than that for Cu. Therefore, for anneal temperatures and total anneal times similar to that of the Cu, we expect that the grain growth of the Cu–Ni will be much slower, and the grain sizes to be smaller. For the 90/10 Cu–Ni alloy foil annealed for 40 min in H_2 followed by growth of graphene in H_2/CH_4, the lateral dimensions of the grains ranged from tens of microns up to a few hundred microns, as seen in Fig. 3. As the growth time increased from 5 to 50 min, the percent of the surface area with grains greater than 100 μm was observed to increase. An analysis of the grain size with growth time is given in Table II. The preferred grain orientation for the 90/10 foils also changed as the growth time increased, as seen in Fig. 3. The grains after the 5 min growth had a variety of surface terminations centered near the (110) orientation. As the anneal time was increased to 50 min, the average grain orientation was observed to shift from the (110) orientation to midway

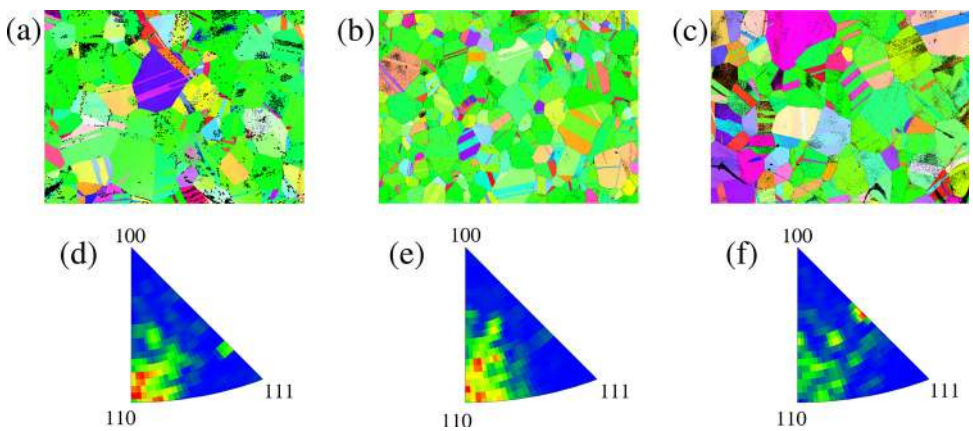

FIG. 3. (Color online) EBSD images of the 90/10 Cu–Ni foils after anneal at 1050 °C for 40 min in 45 mTorr H_2 followed by (a) 5 min (2.3 mm × 1.7 mm), (b) 25 min (3.6 mm × 2.7 mm), and (c) 50 min (2.5 mm × 1.9 mm) in 150 mTorr H_2/CH_4. See Fig. 1 for the EBSD legend. Corresponding inverse pole figures for the 90/10 Cu–Ni foils after growth of graphene for (d) 5 min, (e) 25 min, and (f) 50 min. Orientations are with respect to the surface normal. See Fig. 1 for the density map of the relative areas.

between the (100) and (111) orientations, indicating that the initial (110) orientation is not the most stable surface termination for this alloy. As previously discussed, a likely reason for this could be that the (110) surface is not the lowest energy surface; however, kinetic effects and strain within the film are also expected to play important roles in the evolution of the grain orientation.

IV. DISCUSSION

Our measurements show a (100) texture for the Cu foils after recrystallization at 1035 °C. Wofford *et al*. studied the growth of graphene on 25 μm thick Cu foils with 99.999% purity using low energy electron diffraction (LEED) and low energy electron microscopy (LEEM) and also find a (100) texture for their foils after graphene growth.[34] However, the substrate grains for their foils had a typical lateral dimension of only ~1 mm, and some of the grains in their foil were estimated to be oriented within 0.1° of the [100] surface azimuth. These differences in Cu grain size and orientation can be explained by the higher preanneal and growth temperatures used in our study. As atomic diffusion is a thermally activated process, the diffusion rate is much higher at 1035 °C, which was used for our samples, than at 1000 °C, which was the preanneal temperature used in the LEED/LEEM study. This provides a mechanism for the much larger substrate grains observed under our growth conditions. In addition, the sublimation rate of Cu atoms from the surface during graphene growth is expected to influence the roughness of the surface. At 1035 °C, the sublimation rate is estimated to be as high as 12 ML/s from the bare (100) oriented surface regions of the Cu foil, whereas the rate at 900 °C (the growth temperature used by Wofford *et al*. after the preanneal at 1000 °C) will be no higher than 0.3 ML/s. This and the higher diffusion rate for Cu at our anneal temperature most likely explains the faceted surface structure that we observe with SEM after graphene growth (Fig. 2).

The primary reason that we have studied the growth of graphene on Cu–Ni foils is to allow the controlled growth of graphene films that are more than one atomic layer thick. As Ni surfaces are more catalytically active than Cu surfaces,[35] the rate of dissociation of the hydrocarbon precursor should be much higher than for pure Cu surfaces. In principle, this could mean lower graphene growth temperatures, which would suppress the sublimation of the Cu substrate atoms during growth. In addition, an experimental study of the equilibrium surface composition of Cu–Ni alloy substrates by Sakurai *et al*.[36] has found strong Ni segregation for Cu-rich alloys, which may enhance the catalytic activity further. On the other hand, we observe relatively small, ~100 μm, substrate grains for the 90/10 Cu–Ni foils annealed at 1050 °C. Therefore, either much longer anneal times or higher anneal temperatures are needed to grow centimeter-sized substrate grains, which could be followed by graphene growth at substantially lower temperatures. Because the vapor pressure of Cu is higher than that of Ni, annealing to temperatures near the melting point of the alloy may result in changes in both the bulk and surface alloy compositions of the foil.

For the growth of graphene films with the lowest defect density, it is desirable to have the fewest number of rotational domains during the initial nucleation of the graphene. The ideal situation would be for each grain to nucleate in the same orientation and coalesce into a continuous film without grain boundaries. Recent results for the growth of graphene on Cu single crystal surfaces provide evidence that the substrate orientation can affect the orientation of the graphene overlayer.[35,37,38] For instance, Zhao *et al*. used scanning tunneling microscopy to study graphene films grown on Cu(111) and Cu(100) single crystals by exposing the substrates to 1 mTorr of ethylene for 5 min at 900 °C.[35] The graphene films grown on the Cu(111) substrate had a hexagonal superstructure, whereas the films grown on the Cu(100) substrate had regions with a linear superstructure. The wavelength of the superstructure on the Cu(111) surface is consistent with the formation of a graphene overlayer that is predominantly oriented in the same direction as the Cu(111) substrate. Their LEED measurements for the graphene film grown on the Cu(100) surface show a pattern with a 12-fold symmetry, which indicates that crystallites of graphene are nucleating with two predominant rotational domains, oriented 90° from each other. This result is consistent with what is expected for the growth of a crystal with hexagonal symmetry onto a substrate with square symmetry, especially if both the overlayer and substrate have similar surface lattice constants. The growth of graphene on a Cu(111) surface by evaporation of carbon onto the substrate at temperatures ranging from 690 to 975 °C has been studied by Nie *et al*. using LEEM and μ-LEED.[38] Their results indicate that the in-plane orientation and island morphology of the graphene during growth is strongly dependent on the substrate temperature. At temperatures ≥900 °C, the graphene lattice is closely aligned with the Cu(111) lattice, with all graphene islands aligned to within ±3°.

V. CONCLUSIONS

One of the challenges that must be overcome before graphene can be used in most device applications is the development of methods for producing films with low defect density over wafer-sized dimensions (a few square centimeters). Two factors that are expected to have a large impact on the defect density of the graphene films grown by the dissociation of hydrocarbon molecules on Cu and Cu–Ni substrates are the size and orientation of the metal substrate grains. Our results for graphene growth on cold-rolled Cu foils show that large-area substrate grains can be grown by annealing at a temperature of 1035 °C, which is 48 °C below its melting point. However, the orientation of the surface azimuth of these films is toward the [100] direction, which is not ideal for the growth of low defect density graphene. For the rolled 90/10 Cu–Ni foils, annealing at 1050 °C for up to 90 min resulted in grains with lateral dimensions of a few hundred microns. This result indicates that for the coalescence of grains within the Cu–Ni alloy films to occur, much

higher anneal temperatures are needed. The orientation of the surface normal of the grains of the 90/10 foils under the anneal conditions used in this study was also not in the [111] direction. It is uncertain what the evolution of the grain orientation will be for Cu–Ni alloy foils at much higher anneal temperatures than were used in this study. As the growth of graphene on the (111) surface of Cu or Cu–Ni has the greatest potential for producing films with the lowest defect density, it is advantageous to develop techniques for producing foils of these materials with a (111) surface texture.

ACKNOWLEDGMENTS

This project was supported by the National Science Foundation (Grant No. 1006350/1006411) and the Office of Naval Research. Z.R.R. would like to thank SEMATECH for financial support. In addition, S.S.C. is supported by the China Scholarship Council fellowship, and C.W.M. is supported by the Laboratory Directed Research and Development program at Sandia National Laboratories.

[1]A. K. Geim and K. S. Novoselov, Nat. Mater. **6**, 183 (2007).
[2]A. K. Geim, Science **324**, 1530 (2009).
[3]Y. Zhu, S. Murali, W. Cai, X. Li, J. W. Suk, J. R. Potts, and R. S. Ruoff, Adv. Mater. **22**, 3906 (2010).
[4]C. Lee, X. Wei, J. W. Kysar, and J. Hone, Science **321**, 385 (2008).
[5]J. Lim, W. W. Chen, and J. Q. Zheng, Polym. Test. **29**, 701 (2010).
[6]K. I. Bolotin, K. J. Sikes, Z. Jiang, G. Funkenberg, J. Hone, P. Kim, and H. L. Stormer, Solid State Commun. **146**, 351 (2008).
[7]A. H. Castro Neto, F. Guinea, N. M. R. Peres, K. S. Novoselov, and A. K. Geim, Rev. Mod. Phys. **81**, 109 (2009).
[8]P. R. Wallace, Phys. Rev. **71**, 622 (1947).
[9]K. S. Novosolev, A. K. Geim, S. V. Moreszov, D. Jiang, M. I. Katsnelson, I. V. Grigorieva, V. Dubones, Nature (London) **438**, 197 (2005).
[10]K. Nomura and A. H. MacDonald, Phys. Rev. Lett. **98**, 076602 (2007).
[11]T. Ohta, A. Bostwick, T. Seyller, K. Horn, and E. Rotenberg, Science **313**, 951 (2006).
[12]E. V. Castro, K. S. Novoselov, S. V. Morozov, N. M. R. Peres, J. M. B. Lopes dos Santos, J. Nilsson, F. Guinea, A. K. Geim, and A. H. Castro Neto, Phys. Rev. Lett. **99**, 216802 (2007).
[13]P. Sutter, M. S. Hybertsen, J. T. Sadowski, and E. Sutter, Nano Lett. **9**, 2654 (2009).
[14]A. J. van Bommel, J. E. Crombeen, and A. van Tooren, Surf. Sci. **48**, 463 (1975).
[15]C. Berger, Z. Song, T. Li, X. Li, A. Y. Ogbazghi, R. Feng, Z. Dai, A. N. Marchenkov, E. H. Conrad, P. N. First, and W. D. de Heer, J. Phys. Chem. B **108**, 19912 (2004).
[16]G. G. Jernigan, B. L. van Mil, J. L. Tedesco, J. G. Tischler, E. R. Glaser, A. Davidson III, P. M. Campbell, and D. K. Gaskill, Nano Lett. **9**, 2605 (2009).
[17]J. B. Hannon and R. M. Tromp, Phys. Rev. B **77**, 241404(R) (2008).
[18]R. M. Tromp and J. B. Hannon, Phys. Rev. Lett. **102**, 106104 (2009).
[19]X. Li., W. Cai, J. An, S. Kim, J. Nah, D. Xang, R. D. Piner, A. Velamakanni, I. Jung, E. Tutuc, S. K. Banerjee, L. Colombo, and R. S. Ruoff, Science **324**, 1312 (2009).
[20]X. Li, W. Cai, L. Colombo, and R. S. Ruoff, Nano Lett. **9**, 4268 (2009).
[21]X. Li, Y. Zhu, W. Cai, M. Borysink, B. Han, D. Chen, R. D. Piner, L. Colombo, and R. S. Ruoff, Nano Lett. **9**, 4359 (2009).
[22]X. Li, C. W. Magnuson, A. Venugopal, J. An, J. W. Suk, B. Han, M. Borysiak, W. Cai, A. Velamakanni, Y. Zhu, L. Fu, E. M. Vogel, E. Voelkl, L. Colombo, and R. S. Ruoff, Nano Lett. **10**, 4328 (2010).
[23]X. Li, C. W. Magnuson, A. Venugopal, R. M. Tromp, J. B. Hannon, E. M. Vogel, L. Colombo, and R. S. Ruoff, J. Am. Chem. Soc. **133**, 2816 (2011).
[24]X. Liu, L. Fu, N. Liu, T. Gao, Y. Zhang, L. Liao, and Z. Liu, J. Phys. Chem. C **115**, 11976 (2011).
[25]S. S. Chen, W. W. Cai, R. D. Piner, J. W. Suk, Y. Wu, Y. Ren, J. Kang, and R. S. Ruoff, Nano Lett. **11**, 3519 (2011).
[26]P. Tyagi, R. L. Moore, Z. R. Robinson, C. A. Ventrice, Jr., A. Munson, C. W. Magnuson, and R. S. Ruoff, "X-ray photoelectron spectroscopy study of graphene films grown on Cu and Cu-Ni foils" (unpublished).
[27]M. Hansen and K. Anderko, *Consititution of Binary Alloys* (McGraw–Hill, NewYork, 1958).
[28]O.V. Yazyev and S.G. Louie, Nature Mater. **9**, 806 (2010).
[29]H. Ibach, *Physics of Surfaces and Interfaces* (Springer, Berlin, 2006).
[30]C. S. Barrett and T. B. Massalski, *Structure of Metals* (McGraw–Hill, Elmsford, 1980).
[31]R. E. Honig and D. A. Kramer, RCA Rev. **30**, 285 (1969).
[32]G. Ertl and J. Küppers, *Low Energy Electrons and Surface Chemistry* (Verlag Chemie, Weinheim, 1974).
[33]A. J. Schwartz, M. Kumar, D. P. Field, and B. L. Adams, *Electron Backscatter Diffraction in Materials Science* (Kluwer Academic, New York, 2000).
[34]J. M. Wofford, S. Nie, K. F. McCarty, N. C. Bartelt, and O. D. Dubon, Nano Lett. **10**, 4890 (2010).
[35]L. Zhao, K. T. Kim, H. Zhou, R. He, T. F. Heinz, A. Pinczuk, G. W. Flynn, and A. N. Pasupathy, Solid State Commun. **151**, 509 (2011).
[36]T. Sakurai, T. Hashizume, A. Kobayashi, A. Sakai, S. Hyodo, Y. Kuk. and H. W. Pickering, Phys. Rev. B **34**, 8379 (1986).
[37]L. Gao, J. R. Guest, and N. P. Guisinger, Nano Lett. **10**, 3512 (2010).
[38]S. Nie, J. M. Wofford, N. C. Bartelt, O. D. Dubon, and K. F. MCarty, Phys. Rev. B **84**, 155425 (2011).